

Using ATAN2 it is quite easy to evaluate eq II-12—of course, the same results are obtained either way.

- (12) Petitbois, G. "Tables of Indefinite Integrals"; Dover: New York, 1961.
- (13) Reference 10, Chapter 6.
- (14) Gény, F.; Monnerie, L. *J. Polym. Sci., Polym. Phys. Ed.* 1977, 15, 1.
- (15) In employing the initial condition of eq II-6, we are assuming in the case of "crankshaft-like" motions that all initial conditions have the same Boltzmann factor, i.e., that they are weighted equally. This is an assumption that could yield an unknown error in the resulting correlation function. However,

in passing to the continuum limit embodied in eq II-3, we are assuming the polymer chain is, in some average sense, spatially uniform in the distance scale of motions characteristic of orientational diffusion. It is the spatial uniformity of the chain which provides eq II-6 as the appropriate initial condition. If, in fact, the chain were spatially nonuniform, eq II-6 would be incorrect and an average over the various initial conditions (of unknown weight) would be required. The resulting continuum limit would then be a diffusion equation over a spatially varying (i.e., nonuniform) medium. This would add considerable complexity to the model and would require us to specify much more information about the system than we know.

Damped Orientational Diffusion Model of Polymer Local Main-Chain Motion. 2. Application to Poly(vinyl acetate)

J. Skolnick*,†

Department of Chemistry, Louisiana State University, Baton Rouge, Louisiana 70803

Robert Yaris

Department of Chemistry, Washington University, St. Louis, Missouri 63130.

Received November 9, 1981

ABSTRACT: The damped diffusion model presented in the previous paper is applied to the ^1H NMR relaxation rates and dielectric loss data of poly(vinyl acetate) in toluene. The results are compared to those obtained from the cutoff diffusion model of Bendler and Yaris and the model of Valeur, Jarry, Gény, and Monnerie applied to the same system. The damped and cutoff diffusion models give identical fits to experiment. The model of Valeur et al. also fits the experimental results but only at the expense of nonphysical values for the parameters. A tentative interpretation of the physical origin of the molecular motion is presented.

I. Introduction

In paper 1 a new solvable model for main-chain polymer dynamics was presented.¹ Our model was based upon the Bendler-Yaris model^{2,3} (BY). However, rather than introduce a long-wavelength cutoff to approximate the effects of damping, we incorporated the damping into the motional diffusion equation. The resulting model contains two parameters, β , a damping term, and δ , a term characteristic of the shortest allowable wavelength motions.

In this paper we will fit both the damped diffusion (SY) and the cutoff diffusion (BY) model to Heatley and Cox's measured NMR relaxation rates⁴ for poly(vinyl acetate) (PVA) in toluene- d_8 as a function of temperature and also to Mashimo and Shinohara's dielectric relaxation data,⁵ also for PVA in toluene. We shall compare these results to those obtained by fitting Valeur, Jarry, Gény, and Monnerie's (VJGM) model for main-chain dynamics.^{6,7} Previously, the BY model has been fit to NMR data^{1,8} and the VJGM model has been fit to NMR,^{1,8-12} dielectric,¹³ and fluorescence anisotropy¹⁴ data; but, to the best of our knowledge, this is the first time either model has been fit to both NMR and dielectric data on the same polymeric system. It has previously been stated^{1,8} that both the VJGM model and the BY model fit the data equally well. We shall show that this is not quite the case.

The necessary expressions for the BY and the SY models are in paper 1. For completeness the dipole correlation function in the VJGM model^{6,7} is

$$\phi(t)_{\text{VJGM}} = e^{-t/T_0} e^{-t/T_d} \operatorname{erfc} [(t/T_d)^{1/2}] \quad (1)$$

In this model T_d is supposed to represent the time associated with three-bond "Boyer-crankshaft" motions on a

diamond lattice. The additional exponential decay term with T_0 was introduced⁷ to obtain the proper long-time behavior and T_0 is supposed to represent the time associated with four- (or more) bond motion and diffusive motions.

We remind the reader (see paper 1) that dielectric relaxation measures a vector correlation function, while NMR measures a second-rank tensor correlation function, and that the VJGM, SY, and BY models all predict the equivalence of the normalized first- and second-rank autocorrelation functions. The spectral density is obtained by Fourier transforming eq 1 and is

$$J(\omega)_{\text{VJGM}} = \left[\frac{T_0 T_d (T_0 - T_d)}{(T_0 - T_d)^2 + \omega^2 T_0^2 T_d^2} \right] \times \left\{ \left(\frac{T_0}{2T_d} \right)^{1/2} \left[\frac{(1 + \omega^2 T_0^2)^{1/2} + 1}{1 + \omega^2 T_0^2} \right] + \left(\frac{T_0}{2T_d} \right)^{1/2} \left(\frac{\omega T_0 T_d}{T_0 - T_d} \right) \left[\frac{(1 + \omega^2 T_0^2)^{1/2} - 1}{1 + \omega^2 T_0^2} \right]^{1/2} - 1 \right\} \quad (2)$$

A comparison of the autocorrelation functions for the three models is given in Figure 1. Note that $\phi(t)$ for the VJGM model dies off quickest at long times.

In section II we shall fit these models to the NMR data on PVA.⁴ The fit algorithm is improved¹⁵ over that used in BY (also several misprints have been corrected and the correct expression³ has been used for the relaxation rate T_{AX} , which was in error by a factor of 2). Hence the results presented here for the BY and VJGM models should replace those given in the BY paper. In section III the three models will be applied to the dielectric data on PVA.⁵ Section IV will consist of a discussion summarizing the comparison of the three models' predictions of the NMR

* Present address: Department of Chemistry, Washington University, St. Louis, MO 63130.

Table I
¹H Relaxation Parameters (Methylene = X, Methine = A) for PVA in Toluene-*d*₈ at 300 MHz

Experiment ^a							
temp, °C	T_{AA} , ms	T_{XX} , ms	N_A	N_X			
-45	180	330	-0.9	-0.6			
10	470	270	-0.25	0.08			
30	550	250	0	0			
110	970	400	0.23	0.07			
BY Model ^b							
temp, °C	T_{AA} , ms	T_{XX} , ms	N_A	N_X	ω_A , ^c rad/s	ω_B , ^c rad/s	$R^{c,f}$
-45	202	279	-0.88	-0.61	2.575 + 8	2.574 + 8	3.1 - 3
10	470	270	-0.315	-0.091	2.13 + 7	5.18 + 10	3.4 - 25
30	550	250	-0.062	-0.014	1.01 + 7	3.56 + 10	6.2 - 30
110	970	400	0.063	0.013	1.77 + 8	1.13 + 11	5.2 - 25
SY Model ^d							
temp, °C	T_{AA} , ms	T_{XX} , ms	N_A	N_X	β , ^c rad/s	δ , ^c rad/s	$R^{c,f}$
-45	202	279	-0.88	-0.61	2.54 + 8	4.63 + 6	3.1 - 3
10	470	270	-0.315	-0.091	1.32 + 7	5.21 + 10	8.5 - 32
30	550	250	-0.062	-0.014	6.36 + 7	3.57 + 10	1.1 - 27
110	970	400	0.063	0.013	1.12 + 8	1.11 + 11	7.3 - 27
VJGM Model ^e							
temp, °C	T_{AA} , ms	T_{XX} , ms	N_A	N_X	T_0 , ^c s	T_d , ^c s	$R^{c,f}$
-45	208	282	-0.87	-0.59	3.74 - 9	-1.76 + 32	3.2 - 3
10	486	253	-0.214	-0.56	3.27 - 9	2.98 - 10	5.5 - 4
30	551	246	-0.040	-0.009	1.70 - 9	2.46 - 10	1.6 - 4
110	969	403	0.048	0.010	1.99 - 9	3.19 - 11	1.7 - 5

^a Reference 4. ^b For the BY model, $J(\omega)$ is given by eq II-12 of paper 1. ^c We are using the convention $1.3 - 24 \equiv 1.3 \times 10^{-24}$. ^d For the SY model, $J(\omega)$ is given by eq III-19 of paper 1. ^e For the VJGM model, $J(\omega)$ is given by eq 2. ^f *R* is the sum of the square of the deviations between the theoretical and experimental *T*'s, eq 4. A small value of *R* denotes a very close fit of the model to the experimental values.

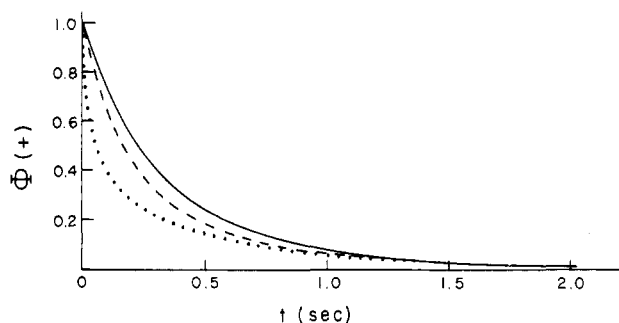


Figure 1. Time dependence of the normalized dipole correlation functions for the damped diffusion model (solid curve), the cutoff diffusion model (dashed curve), and the VJGM model (dotted curve). The parameters were chosen so that the three models would agree exactly at $t = 2$ s (SY: $\beta = 1$, $\delta = 0.216$; BY: $\omega_A = 1$, $\omega_B = 0.1$; VJGM: $T_0 = 1$, $T_d = 0.1$).

and dielectric relaxation spectra of PVA.

II. Fit to NMR Relaxation Rates

Heatley and Cox have measured⁴ the proton–proton relaxation times for both methine (A) and backbone methylene (X) protons (T_{AA} and T_{XX}) for PVA in toluene-*d*₈ at 300.25 MHz. They also reported the Overhauser enhancement factors N_A and N_X for each kind of proton, where

$$\begin{aligned} N_A &= 2T_{AA}/T_{AX} \\ N_X &= 2T_{XX}/T_{XA} \\ T_{AX} &= 2T_{XA} \end{aligned} \quad (3)$$

and T_{AX} is a proton–proton cross-relaxation time. The expressions required to calculate these relaxation times from the spectral density function $J(\omega)/2$ are also given there.¹⁶ These expressions require $J(\omega)$ at several different

frequencies, ω_A , $2\omega_A$, $\omega_A - \omega_X$, $\omega_A + \omega_X$, and $2\omega_X$, where $\omega_A = 300.25$ MHz and $\omega_A - \omega_X = 930$ Hz. Hence the spectral density is probed over a rather wide range of frequencies. For the BY and SY model, we evaluated the spectral density using both the integral and the analytic forms of $J(\omega)$ (eq II-11 and II-12, respectively, of paper 1 for the BY model and eq III-17 and III-19, respectively, of paper 1 for the SY model) as a check. The results are identical with either form. We used the average distances R_{AA} , R_{XX} , and R_{AX} as calculated by Heatley and Cox.⁴ From eq 3 it is apparent that the cross-relaxation time T_{AX} can be experimentally determined in two ways as $2T_{AA}/N_A$ or T_{XX}/N_X . These give different values and are given in Table II of BY (the last column in that table should be headed T_{XX}/N_X). This difference should be kept in mind since theoretically in calculating the Overhauser enhancement factor we only calculate one T_{AX} (from each model).

As was done in BY we fit the two parameters in each of the models by fitting to T_{AA} and T_{XX} at each temperature. We used a nonlinear minimization algorithm,¹⁵ where we minimized

$$R = [T_{AA}(\text{calcd}) - T_{AA}(\text{exptl})]^2 + [T_{XX}(\text{calcd}) - T_{XX}(\text{exptl})]^2 \quad (4)$$

with respect to the two parameters in each of the models. Having a best fit of the parameters, we then calculate T_{AX} and the enhancement factors N_A and N_X , which can be compared to the experiment. The results of this fitting are in Table I.

The first thing that is apparent in Table I is that the -45 °C results are different from any of the others. These are the only experimental results where T_{AA} is less than T_{XX} . None of the models fit the -45 °C results well, and all of them, in the attempt to fit as well as possible, do so

at the cost of a nonphysical parameterization. In the cutoff diffusion model, the short-wavelength cutoff is bigger than the long-wavelength cutoff (or equivalently $\omega_A > \omega_B$). In the damped diffusion model $\beta > \delta$, which is equivalent to the damping length being less than the length of the smallest unit that can diffuse. In the VJGM model, T_d , the time for a three-bond motion, becomes negative and huge. Obviously, the models are all telling us that something significantly different is happening.

In their paper⁵ on the dielectric behavior of PVA in toluene, Mashimo and Shinohara observe a phase transition. The transition temperature is somewhat molecular weight dependent but always occurs considerably above -45°C and considerably below 10°C . They conclude that the high-temperature phase of PVA is quite flexible and in a random coil configuration, while the low-temperature phase is a less flexible, random coil configuration where the motion is quite restrictive. They also conclude that there must be considerable intrachain interactions in the low-temperature phase. None of the models contain such intrachain interactions, and they are telling us that they cannot describe such a situation. Hence we will not discuss the low-temperature phase further—the rest of the paper will deal only with the high-temperature phase.

The second thing that is clear from Table I is that the cutoff diffusion model and the damped diffusion model give exactly the same fit to the NMR relaxation rates. The soft long-range cutoff that the SY model introduces through a damping term is physically more realistic, but clearly both models contain the same essential physics. In this context, it is gratifying that the parameters ω_B of the BY model and δ of the SY model are the same since they are the short-wavelength cutoffs and should remain invariant (if we have correctly treated the basic physics) to what is done at the long-wavelength cutoff. The long-wavelength cutoff β in the SY model is slightly smaller than that in the BY model ω_A as should be the case (remember the cutoff is expressed as a wave vector which is reciprocally related to the wavelength) for a soft rather than a hard cutoff.

The third thing that is clear from Table I is that both the cutoff and damped diffusion models fit the NMR data in a different way from the VJGM model. The BY and SY models have the flexibility to fit both the relaxation rates T_{AA} and T_{XX} exactly—note the extremely small values of R . The VJGM model, while it can certainly fit the relaxation rates to within experimental error, does not have the flexibility to fit the numbers exactly—note the considerably larger values of R . The Overhauser enhancement factors given by all three models are adequate and probably within experimental error, especially considering the two different experimental values of T_{AX} mentioned above and given in Table II of BY.

The rates given in Table I for both the short-range motion and the dissipation (BY: ω_B and ω_A , respectively; SY: δ and β , respectively; VJGM: $1/T_d$ and $1/T_0$, respectively) were fit to an Arrhenius plot and activation energies, E_a , were obtained. These are listed in Table II. Both of the activation energies are the same for our two diffusion models. The activation energy for the dissipation of the diffusive mode is the same as that obtained experimentally⁵ from dielectric relaxation. Furthermore, the activation energy obtained for the short-range diffusive motion, 2 kcal/mol, is characteristic of a single-bond conformational transition.¹⁷ The activation energies obtained from the VJGM model do not agree with the physical interpretation of the model. It does not make physical sense for the activation energy for three-bond

Table II
Activation Energies by NMR Parameterization

model	ϵ_a (short-range motion), kcal/mol	E_a (dissipation), kcal/mol
BY	2.1 ^a	3.9 ^b
SY	2.0 ^c	4.0 ^d
VJGM	5.1 ^e	0.63 ^f
exptl ^g		4.0

^a Arrhenius fit to ω_B . ^b Arrhenius fit to ω_A . ^c Arrhenius fit to δ . ^d Arrhenius fit to β . ^e Arrhenius fit to $1/T_d$. ^f Arrhenius fit to $1/T_0$. ^g Dielectric relaxation ref 5; E_a (kcal/mol).

Table III
Frequency of Maximum Loss Using Parameters Fit to NMR Results for PVA^a in 5% Toluene at 10°C

model	$\log \omega_{\max}$	parameters ^c
exptl ^b	8.6	
BY	10.49	$\omega_A = 2.13 + 7$, $\omega_B = 5.18 + 10$ (rad/s)
SY	10.27	$\beta = 1.32 + 7$, $\delta = 5.21 + 10$ (rad/s)
VJGM	9.30	$T_0 = 3.27 - 9$, $T_d = 2.98 - 10$ (s)

^a The molecular weight is 3.04×10^4 . ^b Reference 5. ^c $2.13 + 7 = 2.13 \times 10^7$ etc.

motion to be 8 times larger than the activation energy for four- (or more) bond motion. In terms of dissipation, if the activation energy for the dissipation of a motion is so much smaller than the activation energy for the motion itself, one would not expect to see the motion.

III. Dielectric Relaxation

In Mashimo and Shinohara's paper⁵ on the dielectric behavior of PVA in toluene, the only temperature that exactly coincides with a temperature at which the NMR was measured is 10°C , so we will only treat that temperature.

We first tried to fit the frequency of maximum loss, ω_{\max} , for the three models using the previously determined NMR parameters. We obtain ω_{\max} by implicitly solving $f(\omega_{\max}) = 0$. The function $f(\omega)$ is given by eq IV-9 of paper 1 for the BY model and by eq IV-18 of paper 1 for the SY model and is obtained from ref 13 for the VJGM model. These results are presented in Table III. While the VJGM model yields an ω_{\max} closer to the experimental result than either of the diffusion models, clearly none of these models is even close to adequate if the NMR parameterization is used. We interpret this negative result in the following way. The models are trying to tell us that there is some essential physical difference between the molecular motions probed by the NMR and the dielectric relaxation. This is not surprising at all since NMR probes a shorter distance scale than does dielectric relaxation. Finally, we note that the fit to ω_{\max} in the SY model gives a fairly good fit to the whole dielectric relaxation curve.

It is clearly pointless to vary both parameters of the models to fit a single experimental number ω_{\max} . Hence we will fit only one parameter of each of the models to ω_{\max} , while keeping the other one fixed at the value obtained by NMR. We then use the resulting parametrized model to predict the maximum loss; i.e.

$$\epsilon''_{\max} = \frac{\epsilon''(\omega_{\max})}{\epsilon_0 - \epsilon_\infty} \quad (5)$$

In the damped diffusion model, it makes physical sense to say the damping term, i.e., the damping length, remains constant. After all, the viscosity of the solvent remains the same and the diffusional mode should damp out over

Table IV
Frequency of Maximum Loss Using a One-Parameter
Fit for PVA^a in 5% Toluene at 10 °C

model	log ω_{\max}	ϵ_{\max}^b	parameters ^d
exptl ^c	8.6	0.31	
BY	8.6	0.363	$\omega_A = 2.13 + 7$, $\omega_B = 1.10 + 9$ (rad/s)
SY	8.6	0.365	$\beta = 1.32 + 7$, $\delta = 1.10 + 9$ (rad/s)
VJGM	8.6	0.329	$T_0 = 3.27 - 9$, $T_d = 2.50 - 9$ (s)

^a The molecular weight is 3.04×10^4 . ^b Defined in eq 5. ^c Reference 5. ^d $2.13 + 7 = 2.13 \times 10^7$ etc.

the same distance scale. In addition, the agreement of the damping activation energy obtained in the NMR parameterization with the measured dielectric relaxation activation energy (see Table II) lends numerical support to our physical considerations. Thus we will keep the damping or dissipative term constant. On the other hand, considering the difference in distances probed by dielectric and NMR relaxation, δ , the short-wavelength cutoff, could be different. Hence we will vary the short-wavelength cutoff and pick the value that gives us the experimental ω_{\max} . Thus in the SY model, β remains at the NMR parameterization while δ is parametrized with respect to ω_{\max} . Similarly, in the BY model we keep the long-wavelength cutoff fixed; hence ω_A remains fixed at the NMR parameterization while ω_B is fit to ω_{\max} . In the VJGM model we shall try to maintain the same physical picture that the parameter representing the dissipative processes remains invariant while the parameter representing the motional unit is allowed to vary. Hence T_d will be fit to ω_{\max} while T_0 is kept at the NMR parameterization. The results of this fitting procedure are in Table IV.

Clearly, all three models fit the experimental value of ω_{\max} and give a good prediction of ϵ''_{\max} . Again, as was the case for the fitting to the NMR relaxation rates, both diffusion models have the same short-wavelength cutoff. The short-wavelength cutoff is considerably longer for the dielectric parameterization than it is for the NMR parameterization. While we cannot obtain these lengths directly since we do not know the chain diffusion constant, we can, however, define the ratio

$$\rho = \left[\frac{\omega_B(\text{NMR})}{\omega_B(\text{diel})_{\text{BY}}} \right]^{1/2} = \left[\frac{\delta(\text{NMR})}{\delta(\text{diel})_{\text{SY}}} \right]^{1/2} = \frac{\lambda_{\min}(\text{diel})}{\lambda_{\min}(\text{NMR})} = 6.9$$

The diffusion constant drops out of the ratio; hence ρ is the ratio of short-wavelength cutoff parameters. It says that the smallest unit that is diffusing is ca. 6.9 times larger in the molecular motion responsible for the dielectric relaxation than it is in the molecular motion responsible for the NMR motion. A possible molecular explanation for the value of ρ can be obtained by realizing that it is the same as the decay length obtained by Skolnick and Helfand (6.72) in their Brownian treatment of conformational transitions.¹⁸ That decay length described the average number of bond lengths before a transforming bond feels no end effects. This suggests the possibility that the molecular motion responsible for the NMR relaxation is a conformational jump motion of single bonds, while the molecular motion responsible for the dielectric relaxation is a motion of persistence length units of length ca. ρ bonds. This interpretation also fits the activation energy for the diffusion (short-range motion) obtained with the NMR parameterization given in Table II. An activation energy of ca. 2 kcal/mol is typical of a single-bond conformational change.

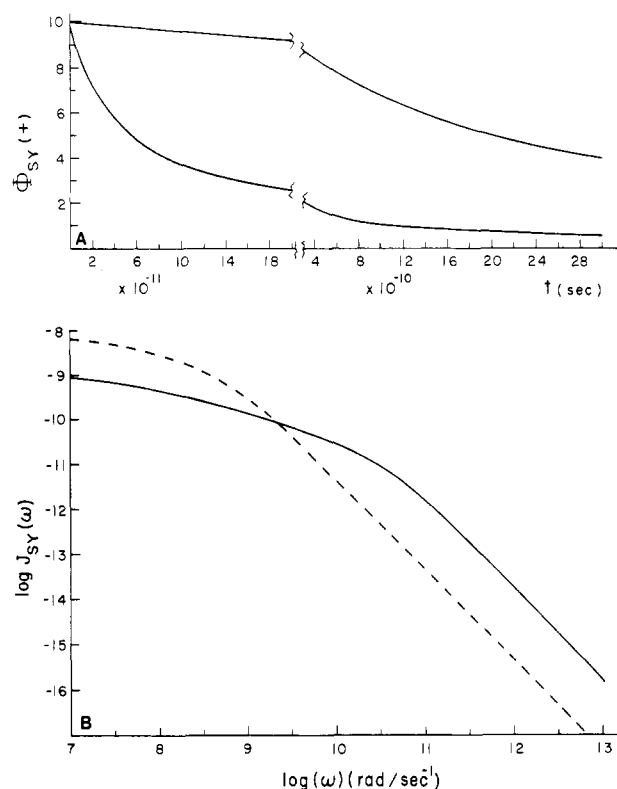


Figure 2. (A) Time dependence of the normalized autocorrelation function for the damped diffusion model. The upper curve is parametrized to fit the dielectric loss of PVA in toluene at 10 °C and the bottom curve is parametrized to fit the proton relaxation rate of PVA in toluene at 10 °C. The cutoff diffusion model gives identical curves on the scale of this graph. (B) Frequency dependence of the spectral density for the damped diffusion model parametrized as in Figure 2A. The dashed line is the dielectric parameterization and the solid line is the NMR parameterization. The cutoff diffusion model gives identical results on the scale of this graph.

When one looks at the dielectric parameterization for the VJGM model, one notices that while T_d is still less than T_0 , they are almost the same, unlike the NMR parameterization, where there is an order of magnitude difference in the times. In the NMR parameterization the physical picture associated with the VJGM model that the molecular motion is essentially three bond makes physical sense in that the rate associated with three-bond motion is an order of magnitude faster than the rate associated with four- and higher bond motions. In the dielectric parameterization where the rates of three-bond and higher bond motion are essentially the same, the physical picture behind the VJGM model has begun to break down, and the interpretation is dubious at best.

We have plotted both the NMR-parameterized and dielectric-parameterized autocorrelation function, Figure 2A, and spectral density, Figure 2B, for the damped diffusion model. On the scale of the graph the similar functions for the cutoff diffusion model would be identical. Similar plots for the VJGM model are presented in Figure 3. It is apparent that there is a much greater difference between the autocorrelation functions (or spectral density functions) in the two parameterizations for the BY and SY diffusion models than there is in the VJGM model. We feel that it is precisely this greater sensitivity of the autocorrelation function (or spectral density) to the parameterization in the diffusion models that allows them to (a) fit the NMR relaxation better than the VJGM model and (b) fit the dielectric data with a physically reasonable set of parameters while the VJGM is forced to fit the dielectric

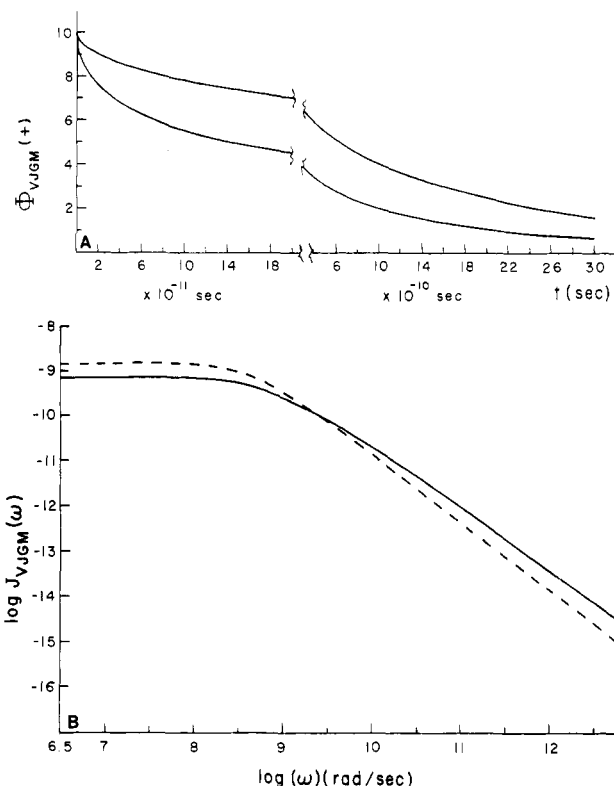


Figure 3. (A) Same as Figure 2A for the VJGM model. (B) Same as Figure 2B for the VJGM model.

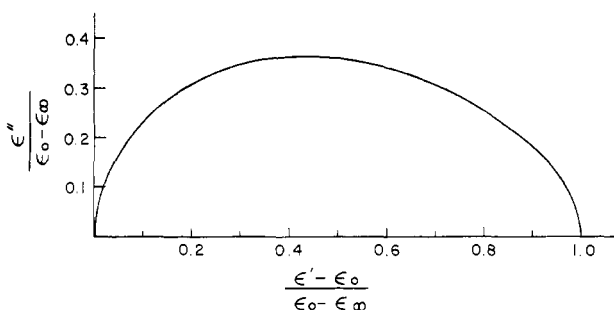


Figure 4. Cole-Cole plot for the damped diffusion model parametrized to the dielectric loss of PVA in toluene at 10 °C. The cutoff diffusion model gives identical results on the scale of this graph.

data with a physically unreasonable set of parameters. One should also note that the limiting slopes of spectra density plots, i.e.

$$\lim_{\omega \rightarrow \infty} \frac{d \log J(\omega)}{d \log \omega}$$

are different in the two models, being -2 in the BY and SY diffusion models and $-3/2$ in the VJGM model.

In Figure 4 we give the Cole-Cole plot¹⁹ for the damped diffusion using the dielectric parameterization model. Again on the scale of the graph the cutoff diffusion model gives an identical Cole-Cole plot.

IV. Discussion

In these two papers we have presented an analytically solvable diffusion model of polymer main-chain motion. This model removes a major physical deficiency of the previous, BY, diffusion model by replacing the ad hoc long-wavelength cutoff by a more physical damping term. It is gratifying to note that the essential physics remained unchanged. Both the hard- and soft-cutoff diffusion models give identical fits to the experimental data. In addition, the short-wavelength cutoffs of the two versions

of the diffusion model remain the same. This indicates that even though the new damped diffusion model is physically preferable and is more amenable to physical interpretation, both the damped and the cutoff diffusion models contain essentially the same physical content.

When we fit the diffusion models to the experimental proton NMR and dielectric relaxation rates of PVA in toluene and compare the diffusion models with the VJGM model we find the following:

(i) The diffusion models can fit the NMR relaxation identically while the VJGM model only "almost" fits them.

(ii) The activation energy for the dissipative term in the diffusion model parameterized to the NMR results is the same as the measured dielectric activation energy (4 kcal/mol), while the activation energy for the diffusive mode is typical of a single-bond conformational transition. On the other hand, the activation energies for the VJGM model do not make physical sense in that they require the activation energy for a three-bond motion to be 8 times as large as for a four-bond motion (or alternatively that the activation energy for the creation of the molecular motion be 8 times as large as that for the dissipation of that motion).

(iii) None of the models parametrized to the NMR experiments could fit the frequency of maximum dielectric loss.

(iv) By keeping the dissipation term constant and reparametrizing the term representing the short-wavelength cutoff, all of the models could fit the dielectric loss data. However, while the diffusion models could fit the dielectric loss data with a physically reasonable (and in fact physically interpretable) set of parameters, the VJGM model required a physically unreasonable set of parameters in order to fit the data.

(v) The agreement between the length ratio of the NMR-to dielectric-parameterized short-wavelength cutoff with a theoretical decay length obtained by Skolnick and Helfand¹⁸ suggests that the diffusive main-chain backbone motion probed by NMR is single bond in character while the motion probed by dielectric loss is the motion of decay length sized units. This interpretation is also consistent with the activation energy obtained for the diffusion mode in the NMR parameterization of 2 kcal/mol, a typical value for a single-bond conformational transition.¹⁷ It will clearly require more investigation on a number of different systems to see whether these agreements are real or fortuitous and whether this interpretation of the results will hold up.

(vi) All of the models required nonphysical values of their parameters in order to fit the low-temperature (-45 °C) phase NMR relaxation rates. It is a good sign that these models all seem to signal when they are breaking down.

In short, the results of this investigation lead to the conclusion that a model of damped diffusive motion is a good phenomenological model for the local motions of the polymer backbone in dilute solution.

Acknowledgment. This study was supported in part by a grant from the Polymer Division of the National Science Foundation (No. DMR-8007025). Acknowledgment is also made to the donors of the Petroleum Research Fund, administered by the American Chemical Society, for partial support of the research. J.S. thanks the Chemistry Department of Washington University for hospitality shown during his visit.

References and Notes

- (1) Skolnick, J.; Yaris, R. *Macromolecules* **1982**, *15*, 1041.
- (2) Bendler, J. T.; Yaris, R. *Macromolecules* **1978**, *11*, 650.

- (3) Errata: Heatley, F.; Bendler, J. T. *Polymer* 1979, 20, 1578.
- (4) Heatley, F.; Cox, M. *Polymer* 1977, 18, 225.
- (5) Mashimo, S.; Shinohara, K. *J. Phys. Soc. Jpn.* 1973, 34, 1141.
- (6) Valeur, B.; Jarry, J. P.; Gény, F.; Monnerie, L. *J. Polym. Sci., Polym. Phys. Ed.* 1975, 13, 667, 675.
- (7) Valeur, B.; Jarry, J. P.; Gény, F.; Monnerie, L. *J. Polym. Sci., Polym. Phys. Ed.* 1975, 13, 2251.
- (8) Jones, A. A.; Robinson, G. L.; Gerr, F. E. *ACS Symp. Ser.* 1979, No. 103, 271.
- (9) Lauprêtre, C. N.; Monnerie, L. *J. Polym. Sci., Polym. Phys. Ed.* 1977, 15, 2127, 2143.
- (10) Heatley, F.; Begum, A. *Polymer* 1976, 17, 399.
- (11) Heatley, F.; Cox, M. *Polymer* 1977, 18, 399.
- (12) Heatley, F.; Begum, A.; Cox, M. *Polymer* 1977, 18, 637.
- (13) Gény, F.; Monnerie, L. *J. Polym. Sci., Polym. Phys. Ed.* 1977, 15, 1.
- (14) Valeur, B.; Monnerie, L. *J. Polym. Sci., Polym. Phys. Ed.* 1976, 14, 11, 29.
- (15) We used a nonlinear least-squares fit: IMSL program ZXSSQ, "IMSL Library Reference Manual", IMSL L1B7-0005, International Mathematical and Statistical Libraries, Inc., Houston, Texas.
- (16) See, however, errata ref 3.
- (17) Flory, P. "Statistical Mechanics of Chain Molecules"; Interscience: New York, 1969.
- (18) Skolnick, J.; Helfand, E. *J. Chem. Phys.* 1980, 72, 5489.
- (19) Cole, K. S.; Cole, R. H. *J. Chem. Phys.* 1941, 9, 341. *Ibid.* 1942, 10, 98.

Some Molecular Motions in Epoxy Polymers: A ^{13}C Solid-State NMR Study

Allen N. Garroway,* William M. Ritchey,[†] and William B. Moniz

Chemistry Division, Naval Research Laboratory, Washington, D.C. 20375, and Chemistry Department, Case Western Reserve University, Cleveland, Ohio 44106.

Received October 8, 1981

ABSTRACT: ^{13}C NMR solid-state spectra have been obtained over the temperature range 150–350 K for four cured epoxy polymers. Each is the diglycidyl ether of bisphenol A (DGEBA) reacted respectively with (i) piperidine, (ii) *m*-phenylenediamine, (iii) hexahydrophthalic anhydride, and (iv) nadic methyl anhydride. These spectra are compared to the spectra of the unreacted DGEBA monomer, in both crystalline and amorphous forms. The polycrystalline DGEBA ^{13}C spectrum suggests that there is more than one monomer conformation or configuration within the unit cell. This is consistent with X-ray structural assignment, which finds that only one stereoisomer is present but that one end of the monomer is slightly disordered so that either of two possible conformations is possible for the epoxide ring. The origins of some of the observed chemical shift splittings are tentatively assigned. The temperature dependence of the spectra of the piperidine-cured epoxy is analyzed. The rotation by 180° of the phenylene rings accounts for the observed coalescence of certain spectral lines. Analysis of the motion by a single relaxation time model suggests a non-Arrhenius process; this behavior is, however, an artifact of the assumption of a single relaxation time. The full temperature dependence is better described by invoking a distribution of correlation times or, equivalently (vide infra), a nonexponential autocorrelation function. The autocorrelation function $\Phi(t) \propto \exp[-(t/\tau_p)^\alpha]$ ($0 < \alpha \leq 1$ and τ_p given by an Arrhenius relation) is used both for these NMR results and for existing dynamical mechanical results for the piperidine-cured epoxy. Analysis with this correlation function is particularly simple in the $\alpha = 0$ limit, as shown. The NMR line shape is critically sensitive to whether the distribution is *inhomogeneous*, arising from a true (spatially varying) distribution of single-exponential processes, or *homogeneous*, with a nonexponential autocorrelation function which describes all common molecular processes and is independent of position. The NMR results are consistent with the activation energy ($E = 63 \text{ kJ/mol}$, 15 kcal/mol) and width parameter ($\alpha = 0.28 \pm 0.02$) found by mechanical spectroscopy, but the 180° flipping of the phenylene ring detected by NMR is either approximately 3000 times slower (inhomogeneous distribution) or 20 times slower (homogeneous distribution) than that for the motion that accounts for mechanical loss. However, the NMR and mechanical relaxation results can be reconciled by presuming that the phenylene rings reorient by small diffusive steps. A reorientation of the phenylene ring by about 3° (inhomogeneous distribution) or 40° (homogeneous distribution) has the same correlation time as the mechanical relaxation process and suggests that small-angle phenylene reorientation occurs with or may be identical with the mechanical relaxation process.

Introduction

The mechanical loss spectrum of a polymer gives a fair overall picture of the frequency and temperature dependence of those molecular motions that couple to an applied stress field. On its own, mechanical spectroscopy does not identify which chemical moieties actually participate in the loss mechanism; such information can sometimes be indirectly inferred from extensive studies¹ of homologous systems. Nuclear magnetic resonance can provide more specific information about the nature of molecular motions. There is, however, no guarantee that motions detected by NMR can actually couple mechanically.

We present here a variable-temperature ^{13}C solid-state NMR study of four epoxy polymers. In the polymers, certain of the resonance lines are found to split below room temperature. In this paper we first examine the origin of these solid-state line splittings. In the solid state, rapid interconversion among many molecular conformations is precluded and resonance lines arise from crystallographically equivalent carbons, rather than chemically equivalent carbons as in the liquid. To refine this point, ^{13}C spectra of four phases of the DGEBA resin are compared: liquid, crystalline, amorphous, and polymerized. A tentative assignment of some of the solid-state splittings in the DGEBA crystal is made by appeal to the crystal structure determined by an X-ray study.² A model for steric hindrance that predicts how the ^{13}C chemical shift is perturbed by crowding of the C–H bonds is used to

* To whom correspondence should be addressed at the Naval Research Laboratory.

[†] Case Western Reserve University